

CHAPTER 57

COMPUTATION OF ALONGSHORE ENERGY

AND LITTORAL TRANSPORT

Theodor R. Mogel¹

Robert L. Street,¹ M. ASCE

Byrne Perry¹

ABSTRACT

This work encompasses a study of the littoral regime of a section of the coastline of the city and county of San Francisco, California. The study included a complete refraction analyses of all applicable deep water wave directions and periods, the determination of breaker locations, and a computation of alongshore energy and potential littoral transport for seven stations located just offshore along the thirty foot depth contour. The waves are refracted from deep water locations to the shoreline using the Stanford Wave Refraction computer program. Wave breaking is assumed to take place whenever the computed wave height exceeds 0.78 times the local water depth. The effect of limiting the refraction coefficient is explored since the refraction theory, in analogy with its parent theory of geometric optics, fails along caustic curves and predicts unreasonably large values for the refraction coefficient.

1 INTRODUCTION

The proper design of coastal structures, improvements or controls depends crucially upon an accurate estimate of the amounts of sand supplied to or lost from the shore region. The most significant portion of the sand supply is the littoral drift--the material of the beach and nearshore bottom moved by the action of waves and currents. The rate and direction of littoral transport or the movement of littoral drift is dependent on many factors, among which are the alongshore components of water-wave energy, currents, availability of littoral drift, its size characteristics, shapes and mineral compositions, tide range, and beach slope. Unfortunately, neither the precise mechanism of transport nor the interaction of the various factors is clearly understood (1-5). The present work is based on the concepts that the principal supply of energy for the movement of littoral drift comes from water waves impinging upon the shore and that an empirical relationship (1,4) between transport and alongshore energy is the most appropriate means for estimating the potential littoral transport.

¹Department of Civil Engineering, Stanford University, Stanford, California 94305

1 1 The Purpose and Scope of the Study

This paper reports on a study (6) of the littoral regime of a section of the coastline of the City and County of San Francisco, California, from the Golden Gate Bridge to Mussel Rock, south of the southerly boundary of the City and County of San Francisco. The original study includes a complete refraction analysis of all applicable deep-water wave directions and periods, determination of the locations of wave breaking, application of 12 monthly tables and an annual table of digitized deep-water wave characteristics (7), calculation of alongshore energy and potential littoral transport, and tabulation of shallow-water wave direction and refraction coefficients for the San Francisco coastline. Here we review the original results and explore the effect of limiting the maximum value that the refraction coefficient can attain (8,11).

1 2 The Plan of the Study

The basic inputs to the study were the hindcast deep-water wave statistics (7) compiled for a deep-water station (number 3, Ref. 7) almost due West from San Francisco. By use of a computer program that carried out a refraction analysis of waves of all applicable periods, heights and directions represented in the wave statistics tables, the deep-water values were carried to seven points distributed in shallow water along the San Francisco shoreline (fig. 1). Then a second computer program computed the alongshore energy components of the waves and, utilizing an empirical relation between these energy components and littoral transport (1,4), computed the monthly and annual potential transport at the seven points on the shoreline. All computations were carried out and plots and printed tables were generated by an IBM 360, Model 67 digital computer with an associated CALCOMP 750 plotter. All programs were written in FORTRAN IV.

The Refraction Program solves the refraction equation and the wave intensity equation along each individual wave ray for arbitrary bottom shapes. The theoretical bases for the computer program were given in detail by Dobson (9) and are discussed briefly below (cf., Ref. 10). The bottom hydrographic data in digitized form and contoured grid maps for two study areas were supplied by the San Francisco Engineer District of the U. S. Army Corps of Engineers. The INNER GRID or study area covered the immediate vicinity of the San Francisco shoreline from Pirates Cove, north of the Golden Gate, to south of Mussel Rock at the southern boundary of the County with a 215 unit by 150 unit grid (333.33 feet per grid unit). The OUTER GRID or study area covered the coast from shore to approximately the 300 fathom contour and approximately from the mouth of the Russian River in Sonoma County to the City of Santa Cruz in Santa Cruz County with a 303 unit by 199 unit grid (1666.67 feet per grid unit) of much greater size. The INNER GRID provided the detailed bottom contours needed for an accurate prediction of wave behavior in shallow water near the coast, while the OUTER GRID provided the link to the deep-water wave conditions. Figures 1a and 1b show CALCOMP (computer) contour plots of the hydrography described by the grids of depths. Waves ranging in period from 4 to 20 seconds and in height from 1 to 25 feet and

coming from directions between North and South-Southeast were considered

The Drift Program utilizes a linear relation between alongshore energy components and potential littoral transport. The alongshore energy components are calculated from output supplied by the Refraction Program and the deep-water wave statistics.

2 METHOD OF COMPUTATION

2.1 Refraction

2.1.1 Theory and Background

The theoretical basis of the present refraction computations is well known (10-12) and will only be touched on here. In effect the same theory is commonly employed in hand computations and only the implementation for the computer led to differences in detail. The original version of the theory comes from the physical science of geometrical optics, the key result of which is Snell's law. A detailed discussion of the method was given by Dobson (9).

The main feature that has been added for the computer work is a technique for fairing a smooth surface through the known bottom depth data. A quadratic surface is constructed to give the best fit in the sense of least squares to the local point and its surrounding neighbors. Thus, the bottom is always represented as a smoothly-varying surface. Starting from a known point on a grid and in a given initial direction, the computer program constructs a single wave ray (or orthogonal) step-by-step across the grid. Because the fitted bottom surface is smooth, and hence differentiable, the equation of wave intensity (equivalently wave height) may be solved at each step in the ray construction process, and the relationship between initial and present wave height carried forward continuously along a single ray. This is an essential feature of the analysis without which the breaking height location computations, described below, would not have been feasible. The refraction technique has proved very satisfactory in many test cases, as shown by comparison with exact theory and hand computations (9). Battjes (13) has recently shown that, according to both linear and nonlinear theory, the energy flux in wave propagation in three dimensions is always directed along the wave rays (orthogonals) [our wave intensity equation is based on this fact] regardless of the wave amplitude gradients and that refraction of water waves over bottoms of small slope can indeed be considered as a case of wave propagation through an inhomogeneous (depth varies), two-dimensional medium. This is in agreement with the method used in the present work and current practice.

The refraction theory, in analogy with its parent theory of geometric optics, fails along caustic curves and predicts unreasonably large values for the refraction coefficient K_r near the caustic curve. Pierson (8,11) gave justification for the approximate limit $K_r^2 \leq 2.0$ and we have run test cases for $K_r^2 \leq 2.0$, $K_r^2 \leq 4.0$, and $K_r^2 < \infty$.

2.1 2 Technique

The refraction program constructed rays on either the OUTER GRID (303 x 199 grid units) or the INNER GRID (215 x 150 grid units). The depth data at the intersection points of the grids was provided by the San Francisco Engineer District and was digitized from their bottom hydrography charts. A match line for transfer of computations from one grid to the other was established.

The calculation of littoral transport requires the shallow-water wave height and direction at the point of breaking of every possible wave in the three-dimensional matrix of deep-water statistics (parameterized by deep-water height, direction and period). Accordingly, on an inward run from deep to shallow water, the refraction program punched a data card whenever breaking occurred on the INNER GRID, only those breaking points near the beach were retained. For the range of wave heights and periods considered in this study, breaking was assumed to occur whenever the height of a particular wave exceeded 0.78 times the local water depth. While more sophisticated criteria are available (12), it appears that none is significantly more accurate on the average for prototype waves in our period range. Furthermore, in view of the basis of the refraction analysis on linear theory, a more refined breaking criteria does not appear warranted.

The objective of the refraction analysis was to bring one ray from deep water to each of the seven target points near the shore for each applicable deep-water direction and period. Because local wave height is a linear function of deep-water height, all the results for the heights between 2 and 24 feet were obtained from a single ray computation. In view of the complex hydrography of the San Francisco shore region, it was decided to work outward from each target station with fans of rays, the rays in each fan having a different period. New fans were generated until a set of results were obtained in deep water that would permit us to run a complete set of applicable waves in from deep water (corresponding to the wave statistics). It was not possible to generate the necessary data on an outgoing run because the refraction coefficient calculation is not valid for rays started in shallow water (the starting condition of parallel rays is not correct there). Therefore, it remains necessary to retrace outgoing rays from deep water inward. In some cases it was possible to begin with incoming rays of specific period and direction and to hit a target station by using trial-and-error and the information known about adjacent stations.

A study of the hindcast data (7) shows that the wave statistics are given for 22.5-degree direction segments, two-second period intervals and two-foot height intervals. We used the mid-direction, mid-period and mid-heights in our refraction calculations. In light of the difficulty of hitting a given direction with an outward running ray or a given station with an inward ray we established tolerance criteria of ± 5 degrees on direction when running outward and an x-distance tolerance of ± 4 grid units when running in. Tests of the results showed that no large changes in wave characteristics occurred within these tolerances. In any case the majority of the runs are well within the tolerance limits which seem reasonable in view of the expected accuracy of the hindcast deep-water statistics.

2 1 3 Notes on Computer Programming

The results of the present study were obtained on an IBM 360/67 digital computer and an off-line CALCOMP 750 plotter. The program is an extension of the Stanford Refraction Program originally developed for the IBM 7090. Dobson (9) has given a very thorough documentation including flow charts for the main program and subroutines in the original program, except for the CALCOMP subroutine calls which are highly installation dependent.

The primary changes made in the original Stanford Program have been related either to differences between the IBM 7090 and IBM 360/67 computers or improvements in the graphical displays and printed or punched outputs of the program.

For the present study the program has been specifically modified to do the following:

- a Read the Depth data and associated fixed grid and ray constants and identifiers from Disc storage in the machine.
- b Plot wave rays on a map (Fig 1). The map includes labeled X and Y axes, a north direction arrow, suitable contours (stored on Disc also), and identification block giving relevant parameters and identification. The contours on the INNER GRID are the shoreline and 30-foot contours, while only the shoreline is shown on the OUTER GRID. If the ray is to continue to another grid, the map also shows the match line outline of the next grid.
- c Create a punched card data deck to continue wave rays on another grid. The X- and Y-coordinates in the data deck have been converted to the new coordinate system. The data deck is complete with all necessary title and end-of-set cards so that it may be loaded for the next run without further processing.
- d Create a punched-card data deck giving coordinates and wave parameters at the 30-foot contour for each wave ray.
- e Create a punched-card data deck with one card for each deep-water wave height on each ray when the wave breaks ($H/D > 0.78$) for heights of 2 to 24 feet in increments of 2 feet. These cards contained, in addition to the wave height, direction, period and spacial location, the shoaling coefficient, the deep-water height, the water depth and the local angle between the wave ray and the gradient of the bottom topography.
- f Limit the refraction coefficient to a specific value.

Figures 1a and 1b show sample plotter output from the refraction program. A ray was started a short distance to each side of each of the actual rays used to better illustrate the shifting of the wave front. Tables 1a and 1b are the printouts generated for one of the rays shown in the figures.

2.2 Littoral Transport

2.2.1 Analysis and Hindcast Data

National Marine Consultants compiled deep-water wave statistics based upon meteorological records and charts for the years 1956, 1957 and 1958 for seven deep-water stations along the California coast (7). The wave hindcast data for deep-water sea (generated by local wind) and swell were given as height-period-direction average frequency distributions in percent monthly and annually. A digitized data deck for Station 3 (Latitude 37.6 degrees N, Longitude 123.5 degrees W) was provided the authors by the San Francisco Engineer District. This station is due west of San Francisco. As none of the other stations were close to this area, Station 3 was the only data source, cf., Fairchild (3) who interpolated between several stations for an east-coast study.

The treatment of deep-water wave statistics and littoral transport calculations was based on the methods of Saville (14) and Fairchild (3). In particular, sea and swell energies were added linearly, and the significant wave heights, corrected in accordance with Fairchild (3) and Saville (14), were used to estimate the wave energy at the shore. The refraction analysis used the dominant wave period, as outlined by Saville (14), associated with the significant wave heights given in the statistical data.

Littoral transport was computed from the alongshore energy components derived from the combination of wave statistics and refraction program output for the seven shallow-water stations shown in Fig. 1b. An empirical littoral transport equation was obtained from Fig. 2-22 of CERC Technical Report No. 4 (1). According to this figure, the potential littoral transport past a point on shore and caused by a given period wave of given deep-water height and direction is

$$Q = 128 E_a \cdot 10^{-6} \text{ cu yds/month}$$

where

$$E_a = 0.58 E_{aF} \cdot |j_k|,$$

$$E_a = 5400 \frac{\gamma H_b^2 L_o}{TK_s} \sin \alpha_c \cos \alpha_c = 1.77 \cdot 10^6 \frac{H_b^2 T}{K_s} \sin \alpha_c \cos \alpha_c$$

in ft-lbs/ft of beach/day,

α_c = angle between wave ray and the gradient of the bottom hydrography in degrees,

γ = specific weight of sea-water = 64 lbs/ft³,

H_b = shallow-water wave height at breaking in feet,

T = wave period in seconds,

K_s = the shoaling coefficient at breaking,

L_o = the deep-water wave length in feet = $5.12T^2$

F_{ijk1} = WAVES (I,J,K,L) = fraction of a month that waves of given height, period, direction and month occur in deep water = (percent per month) (days per month)/100

The actual (as opposed to potential) littoral transport may be less than Q if bottom bed material is not available at the point in question. The factor 0.58 is required (14) to reduce the given deep-water spectral energy for significant waves to the proper average energy that causes littoral transport. Note that in this analysis the littoral transport caused by waves of varying heights will occur where the wave breaks, thus, for each station location our transport results reflect the alongshore transport on the average through the broad-band breaking or surf zone (see Fig. 4) created by a set of deep-water waves whose common point is that they all pass through (or near) a given station location (1 through 7) on the 30-foot contour along the San Francisco shoreline.

The machine calculations were checked by hand for those cases in which only one deep-water wave height for a given period and direction had a nonzero occurrence in a month or for the year.

2.2.2 Programming and Output

The operation of the program that calculates the alongshore energy and potential littoral transport is particularly simple and proceeds as follows:

- a The program reads the digitized sea data (Table 3, Ref. 7) and constructs WAVES (I,J,K,L) for the sea data for each month.
- b The program reads the swell data and adds it to the appropriate WAVES (I,J,K,L).
- c The program reads a refraction-program-punched input card for a particular deep-water height, direction, period and station (always starting with the 24-foot height and working downward) and constructs E_a for that card. Cards are read and energies calculated until all the heights for a given ray are surveyed, and their energies are added together to find the total energy for that period and direction. Only the last complete height survey (24 feet to 2 feet) is used to calculate the transport, i.e., only the breaking zone contiguous to the beach is considered to cause transport. No allowance has been made for energy losses in prior breaking zones away from the beach (see Sec. 4.2).
- d The program repeats c for the remaining periods and directions.

- e The littoral transports Q corresponding to the E_a^{\sim} for each period and direction are computed
- f Tables of E_a^{\sim} and Q are constructed for each station

3 RESULTS AND DISCUSSION

3.1 Transport and Energy Tables

The tables of littoral transport and alongshore energy components computed by the Drift Program for the three limits on K_r are given in Tables 2 and 3 for each of the seven stations of the study. Results are given for each month in the year and the annual total transport as a station. A positive sign indicates energy components and transport motion up-coast or generally North.

As noted above (Secs. 2.1.3 and 2.2.1) the alongshore energy component computation is based upon the local angle α_c at breaking between the wave ray and the gradient of the bottom hydrography (the perpendicular to the local bottom contour). We considered the use of the mean gradient direction of the beach as a whole near any given station in lieu of the local gradient. Tests with this concept had predictable results, namely, the transport and energy components vary widely for small changes in mean beach gradient direction. Because of the complex hydrography near the shore (Fig. 1b) and the wide zone of breaking (Fig. 2) the direction of a ray at the breaking point for a given wave is not correlated to any observable mean beach gradient direction. Accordingly, no computations utilized an α_c based on mean beach gradients; rather, the ray direction was correlated with the bottom contour at the actual breaking point.

As can be seen from the alongshore energy and littoral transport tables (Tables 2, 3, & 4), limiting the maximum value of K_r tends to make the calculated energy and transport more uniform. The majority of the alongshore energy at each station is the result of a few rays. When some of these rays pass through or near a caustic and their K_r is not restricted, their dominance is exaggerated and they break further from shore. By limiting the maximum value that K_r can attain, the dominance of these waves is reduced and they break closer to the beach zone. Station 1, for example, has a ray from the west which contributes most of the energy and transport. When this ray crosses the 30 ft contour $K_r = 3.67$. When K_r is restricted to a more reasonable value, the dominance of the ray diminishes and the net transport is brought into line with the transport of station 3 as expected because the bottom hydrography near these two stations is similar.

3.2 Unusual Features

Several features of the bottom hydrography are worth noting. The Farallon Islands are the visible portion of a shoaling region which lies mainly between 60 fathoms and the surface. Long waves, in particular, are affected by this region. The peaked nature of the region causes bending of the longer waves which is quite unpredictable and led to much of the tedium of locating the starting positions of these longer waves.

The Fourfathom Bar blocks or diverts much of the wave energy of the longer period waves from the Golden Gate area. The small energy and transport figures for stations 6 and 7 are a direct result of this blocking effect. The Southern and Central portions of the San Francisco Bar also severely bend the rays. However this effect is quite predictable.

3 3 Comparison with other studies

Kamel (15) made a study of sand transport along the California Coast in the Russian River-Point San Pedro reach using, mainly, radioactive tracer and heavy mineral concentrations. His study predicts a general transport in the southerly direction. In the region between the Golden Gate and Merced Lake (our stations 4 and 2) no predominant direction of transport was predicted and the radioactive tracer samples predicted a Southern transport near our stations 1 and 3. However a close examination of the heavy mineral concentration data for the same region shows a Northern transport for the same region.

Adding to the uncertainty Johnson (16) states in his study of the Half Moon Bay-Russian River region that little if any material is transported in this littoral zone. Our results indicate, with the exception of station 2, a northerly direction of sand transport. Johnson (16) also concludes that there is no major source of littoral materials along the Half Moon Bay-Russian River region indicating that perhaps the experimental results revealed not what is taking place now but what has taken place over geologic time.

4 Conclusions

4 1 Conclusions based on the present results

In this study we brought together three essential ingredients to synthesize the potential littoral transport and alongshore energy. The combination of deep-water hindcast wave statistics, linear refraction of wave components and an empirical relation between energy and transport produced energy and transport patterns which clearly show that

- 1) The average annual transport and energy direction is north
- 2) The Farallon Islands and their associated shoaling region both block wave energy from the shore and bend and focus wave rays to zones not otherwise reachable
- 3) Limiting the maximum value of K_p produces energy and transport predictions which are more uniform and realistic

However it must be emphasized that the littoral transport results are obtained from an empirical energy-transport relation developed for other coastal areas and based on very scattered data (4,5). Accordingly, within the accuracy of the hindcast data and the linear refraction analysis, we consider the alongshore energy distribution to be accurate, but the potential (computed) littoral transport can only be considered as a qualitative indicator of the actual transport.

4.2 Recommendations for Modification of the Present Technique

Three problem areas arise in connection with the present study. First, a large effort in terms of man-hours and computer time is expended in selecting the desired wave rays for each deep-water wave direction and period that run to each station. Second, and more significant, no account is made of energy losses that occur through wave breaking on bars and other shoaling regions far from the beach area. Third, the relationship between energy and sand movement rests on little in the way of sound principles and analysis. Thornton (5) has recently made a start in remedying this situation, but his success is limited.

Battjes (13) proposes a refraction technique in which the wave characteristics are determined as continuous field variables over an entire grid. This method requires the solution of a pair of non-linear partial differential equations, but would give the necessary data at all points along a shoreline. However his method would require large amounts of storage ($\sim 10^6$ words for our Outer Grid) and long run times (probably more than 10 minutes per wave direction and period). Our present program has none of these problems.

The greatest need, however, is to find a way to account for energy loss when a wave breaks offshore before coming into the breaker zone. Battjes (13) technique assumes no energy losses from the wave system so would suffer from some of the present inaccuracies.

ACKNOWLEDGEMENT

The basic refraction and littoral drift studies were carried out under Contract No. DACW07-68-C-0054 for the U. S. Army Engineer District, San Francisco, Corps of Engineers.

REFERENCES

- 1 Shore Protection, Planning and Design, Tech Rep No 4 (3rd ed), U S Army Coastal Engineering Research Center, Dept of the Army, Corps of Engineers, Washington, D C , June 1966
- 2 J W Johnson and P S Eagleson, "Coastal Processes," Estuary and Coastline Hydrodynamics, McGraw-Hill Book Co , Inc , New York, Chapter 9, 1966
- 3 J C Fairchild, "Correlation of Littoral Transport with Wave Climate along Shores of New York and New Jersey," Tech Memo No 18, U S Army Coastal Engineering Research Center, Dept of the Army, Corps of Engineers, Washington, D C , November 1966
- 4 T Saville, Jr , G M Watts, " Coastal Regime, Recent U S Experience," XXII International Navigation Congress, Paris, 1969
- 5 E B Thornton, "Longshore Currents and Sediment Transport," Tech Rep No 5, Department of Coastal and Oceanographic Engineering, University of Florida, Gainesville, Florida, December, 1969
- 6 Street, R L , T Mogel and B Perry, "Computation of the Littoral Regime of the Shore of San Francisco County, California, by Automatic Data Processing Methods," Final Report, Contract No DACW07-68-0054, U S Army Engineer District, San Francisco, Corps of Engineers, 1 January 1969
- 7 "Wave Statistics for Seven Deep Water Stations Along the California Coast," National Marine Consultants, Santa Barbara, California, December 1960
- 8 W J Pierson, "The Interpretation of Crossed Orthogonals in Wave Refraction Phenomena," Tech Memo No 21, Beach Erosion Board, Corps of Engineers, January 1951
- 9 R S Dobson, "Some Applications of a Digital Computer to Hydraulic Engineering Problems," Tech Rep No 80, Dept of Civil Engineering, Stanford University, Stanford, California, June 1967, DDC AD No 659309
- 10 G H Keulegan, J Harrison, "Tsunami Refraction Diagrams by Digital Computer," J Waterways and Harbor Division, Proc ASCE, V96, No WW2, Paper 7261, May 1970
- 11 W J Pierson, G Neumann and R W James, Practical Methods for Observing and Forecasting Ocean Waves by Means of Wave Spectra and Statistics, U S Navy Hydrographic Office, Publication No 603, 1955

- 12 R L Wiegel, Oceanographical Engineering, Prentice-Hall, Inc , Englewood Cliffs, New Jersey, 1964
- 13 J A Battjes, "Refraction of Water Waves," J Waterways and Harbor Division, Proc ASCE, V 94, No WW4, Paper 6206, November 1968
- 14 T Saville, Jr , "North Atlantic Coast Wave Statistics Hindcast by Bretschneider-Revised Sverdrup-Munk Method," Beach Erosion Board Tech Memo No 55, Dept of the Army, Corps of Engineers, Washington, D C , November 1954
- 15 A M Kamel, "Littoral Studies Near San Francisco Using Tracer Techniques," Tech Memo No 131, Beach Erosion Board, November 1962
- 16 J W Johnson, "Nearshore Sediment Movement--Central California Coast," Coastal Engineering, ASCE Santa Barbara Specialty Conference, Chapter 23, October 1965

TABLE 1A OUTER GRID COMPUTER PRINTOUT SAMPLE

SAN FRANCISCO				OUTER GRID				DATE			
SET NO 1, PERIOD = 13 00 SECS, RAY NO 36, TIME STEP = 18 7823 SECS								9/11/70			
PCINT	X (GU)	Y (GU)	ANGLE (DEG)	DEPTH (FT)	MAX DIF (PERCENT)	LENGTH (FT)	SPEED (FPS)	KR KS	KR DIMENSIONLESS	KS	B2
1	136 88	188 20	-110 50	1805 99	0 00	865 35	66 57	1 00	1 0000	1 0000	1 0000
30	129 26	167 83	-110 50	1805 99	0 00	865 35	66 57	1 00	1 0000	0 9954	1 0004
60	121 38	146 75	-110 46	494 91	1 57	864 05	66 47	1 00	1 0000	0 9388	1 5046
90	114 52	125 84	-103 59	233 24	0 57	818 46	62 96	0 77	0 8234	0 9180	3 0296
120	111 64	105 33	-93 31	172 90	1 45	768 62	59 12	0 53	0 5772	0 9149	-0 6283
150	111 66	86 28	-88 91	119 77	0 94	689 85	53 07	1 33	1 4559	0 9641	-4 2963
180	113 12	70 10	-77 81	64 04	0 35	544 15	41 86	0 47	0 4849	0 9770	-4 4334
* 183	113 41	68 73	-77 77	58 05	2 73	522 16	40 17	0 47	0 4774	1 0891	-4 1109
210	115 21	59 26	-79 49	30 65	2 65	393 05	30 23	0 54	0 4957	1 1904	-0 6427
240	118 24	50 73	-72 80	19 82	6 14	320 38	24 84	1 05	0 8825	1 6461	6 0813
270	117 86	44 39	-116 34	4 86	50 56	161 58	12 43	0 64	0 3895	1 6984	-7 0683
300	116 83	41 46	-108 34	0 65	229 16	39 31	4 58	2 22	0 4525	7 6085	-7 3857
RAY STOPPED, REACHED SHORE				X = 116 58, Y = 41 08		35 34	0 37	2 81			

TABLE 1B INNER GRID COMPUTER PRINTOUT SAMPLE

SAN FRANCISCO				INNER GRID				DATE			
SET NO 1, PERIOD = 13 00 SECS, RAY NO 36, TIME STEP = 3 7557 SECS								9/11/70			
PCINT	X (GU)	Y (GU)	ANGLE (DEG)	DEPTH (FT)	MAX DIF (PERCENT)	LENGTH (FT)	SPEED (FPS)	KR KS	KR DIMENSIONLESS	KS	B2
1	47 02	142 80	-95 67	90 76	1 76	865 35	66 57	1 00	1 1377	0 9274	0 7740
20	46 59	132 45	-87 13	92 76	1 90	430 15	48 47	1 06	1 1524	0 9333	0 7524
40	47 10	121 72	-85 28	85 91	1 90	610 12	47 09	1 08	1 1574	0 9384	0 7455
60	47 59	111 25	-94 16	81 03	0 42	598 37	46 03	1 09	1 1875	0 9471	0 7081
80	49 12	101 06	-92 78	74 25	0 78	578 03	44 46	1 12	1 1875	0 9709	0 6910
100	50 65	91 54	-79 39	60 76	0 40	532 33	40 95	1 17	1 2022	0 9900	0 6957
120	52 44	82 73	-77 43	53 05	0 51	502 43	38 65	1 19	1 2007	1 0171	0 7388
140	54 47	74 58	-75 19	44 75	0 54	466 45	35 88	1 19	1 1656	1 0509	0 8154
160	56 47	67 01	-75 76	37 09	0 43	428 85	32 99	1 17	1 1103	1 0575	0 8239
* 162	56 65	66 29	-76 12	35 83	0 57	422 18	32 48	1 17	1 1046	1 0759	0 8369
* 165	56 50	65 23	-77 16	32 67	0 89	404 75	31 13	1 18	1 0960	1 0977	0 8468
* 167	57 05	64 56	-78 21	29 43	0 61	385 73	29 07	1 20	1 0900	1 0759	0 8468
* 186	57 12	64 23	-78 85	27 56	0 65	374 17	28 78	1 21	1 0867	1 1120	0 8523
* 170	57 23	63 60	-80 45	25 45	0 33	346 97	26 69	1 24	1 0793	1 1491	0 8655
* 171	57 28	63 31	-81 32	23 56	0 37	331 94	25 53	1 26	1 0749	1 1717	0 8730
* 173	57 32	62 76	-82 13	21 81	0 41	307 77	24 29	1 28	1 0763	1 1921	0 8811
* 175	57 41	62 76	-85 13	16 23	0 73	287 77	23 44	1 32	1 0763	1 2431	0 8940
* 177	57 41	61 81	-82 60	13 22	0 53	263 80	22 29	1 37	1 0560	1 3014	0 9094
* 177	57 45	61 81	-82 71	10 54	0 66	236 35	18 18	1 44	1 0471	1 3704	0 9190
* 180	57 48	61 23	-87 17	8 03	12 68	206 95	15 92	1 51	1 0361	1 4601	0 9371
* 181	57 49	61 05	-87 65	7 46	13 65	199 57	15 35	1 53	1 0330	1 4858	0 9425
* 190	57 50	59 61	-92 02	4 10	10 64	148 62	11 43	1 73	1 0081	1 7147	0 9885
* 190	57 47	59 07	-94 50	-0 25	-652 48	87 09	6 70	2 23	0 9985	2 2327	1 0056
TOPPED, REACHED SHORE				X = 57 47, Y = 59 07							

TABLE 2 ALONGSHORE ENERGY FOR $K_r < \infty$ (10^6 ft-lbs/ft of beach)

STATION	1	3	2	5	4	6	7
JAN	3489	1452	4180	22092	5031	666	225
FEB	4625	3114	8302	21418	8030	244	1084
MAR	2167	1180	2705	10584	2583	-9	4
APR	769	824	-39	5195	2642	2617	177
MAY	104	347	-261	1253	1271	-143	169
JUN	-429	-80	-247	-1717	75	-3	1
JUL	-361	-56	-90	-1163	34	-5	2
AUG	-411	-45	-182	-1043	35	23	2
SEP	-92	110	152	-27	349	-20	7
OCT	305	226	297	1206	1049	384	70
NOV	982	89	88	2669	839	1081	-5
DEC	1866	603	1009	5857	1430	1171	-14
TOTAL	13014	7764	15914	66324	23368	6006	1722

POTENTIAL LITTORAL TRANSPORT FOR $K_r < \infty$ (10^3 cubic yards)

STATION	1	3	2	5	4	6	7
JAN	447	186	535	2828	644	86	29
FEB	592	399	1063	2741	1027	31	139
MAR	277	151	346	1355	331	-1	1
APR	98	105	-5	665	338	335	23
MAY	13	44	-33	160	163	-18	22
JUN	-55	-10	-32	-220	10	0	0
JUL	-46	-7	-12	-149	4	1	0
AUG	-53	-6	-23	-134	4	3	0
SEP	-12	14	20	-4	45	-3	1
OCT	39	29	38	154	134	49	9
NOV	126	11	11	342	107	138	-1
DEC	239	77	129	750	183	150	-2
TOTAL	1665	993	2037	8488	2990	770	221

TABLE 3 ALONGSHORE ENERGY FOR $K_r \leq 2$ (10^6 ft-lbs/ft of beach)

STATION	1	3	2	5	4	6	7
JAN	3029	1440	-184	6701	3708	21	225
FEB	3719	3006	199	7888	6822	319	1084
MAR	1410	1097	-616	1963	1564	35	4
APR	392	789	156	1420	2001	579	177
MAY	-196	342	-185	-806	462	12	169
JUN	-556	-80	-198	-1722	75	37	1
JUL	-435	-56	-67	-1162	34	9	2
AUG	-469	-45	-182	-1044	35	37	2
SEP	-251	107	-192	-496	166	30	7
OCT	13	211	-594	-49	458	-18	70
NOV	179	89	-644	-304	330	-49	-5
OEC	943	562	-1673	925	881	-28	-14
TOTAL	7778	7462	-4179	13314	16536	984	1722

POTENTIAL LITTORAL TRANSPORT FOR $K_r \leq 2$ (10^3 cubic yards)

STATION	1	3	2	5	4	6	7
JAN	388	184	-24	858	475	3	29
FEB	476	385	26	1010	873	41	139
MAR	180	140	-79	251	200	4	1
APR	50	101	20	182	256	74	23
MAY	-25	44	-24	-103	59	2	22
JUN	-71	-10	-25	-221	10	5	0
JUL	-56	-7	-9	-149	4	1	0
AUG	-60	-6	-23	-134	4	5	0
SEP	-32	14	-25	-63	21	4	1
OCT	2	27	-76	-6	59	-2	9
NOV	23	11	-82	-39	42	-6	-1
OEC	121	72	-214	118	113	-4	-2
TOTAL	996	955	-535	1704	2116	127	221

TABLE 4 ALONGSHORE ENERGY FOR $K_r \leq 1.41$ (10^6 ft-lbs/ft of beach)

STATION	1	3	2	5	4	6	7
JAN	3200	1357	6	3233	2921	168	128
FEB	3130	2537	1477	5295	4478	346	625
MAR	902	792	-496	882	1229	83	-9
APR	260	583	-243	-13	1426	60	101
MAY	-342	295	-171	-961	294	61	92
JUN	-593	-80	-190	-1712	75	53	1
JUL	-456	-56	-63	-1160	34	15	2
AUG	-486	-45	-182	-1041	35	45	2
SEP	-327	67	-159	-499	133	60	4
OCT	-237	163	-446	-334	353	64	34
NOV	-179	89	-578	-468	273	62	-8
DEC	642	434	-1902	228	739	133	-19
TOTAL	5514	6136	-2947	3450	11990	1150	953

POTENTIAL LITTORAL TRANSPORT FOR $K_r \leq 1.41$ (10^3 cubic yards)

STATION	1	3	2	5	4	6	7
JAN	410	174	1	414	374	22	16
FEB	401	325	189	678	573	44	80
MAR	115	101	-64	113	157	11	-1
APR	33	75	-31	-2	183	8	13
MAY	-44	38	-22	-123	38	8	12
JUN	-76	-10	-24	-219	10	7	0
JUL	-58	-7	-8	-149	4	2	0
AUG	-62	-6	-23	-133	4	6	0
SEP	-42	9	-20	-64	17	8	1
OCT	-30	21	-57	-43	45	8	4
NOV	-23	11	-74	-60	35	8	-1
DEC	82	56	-243	29	95	17	-2
TOTAL	706	787	-376	441	1535	149	122

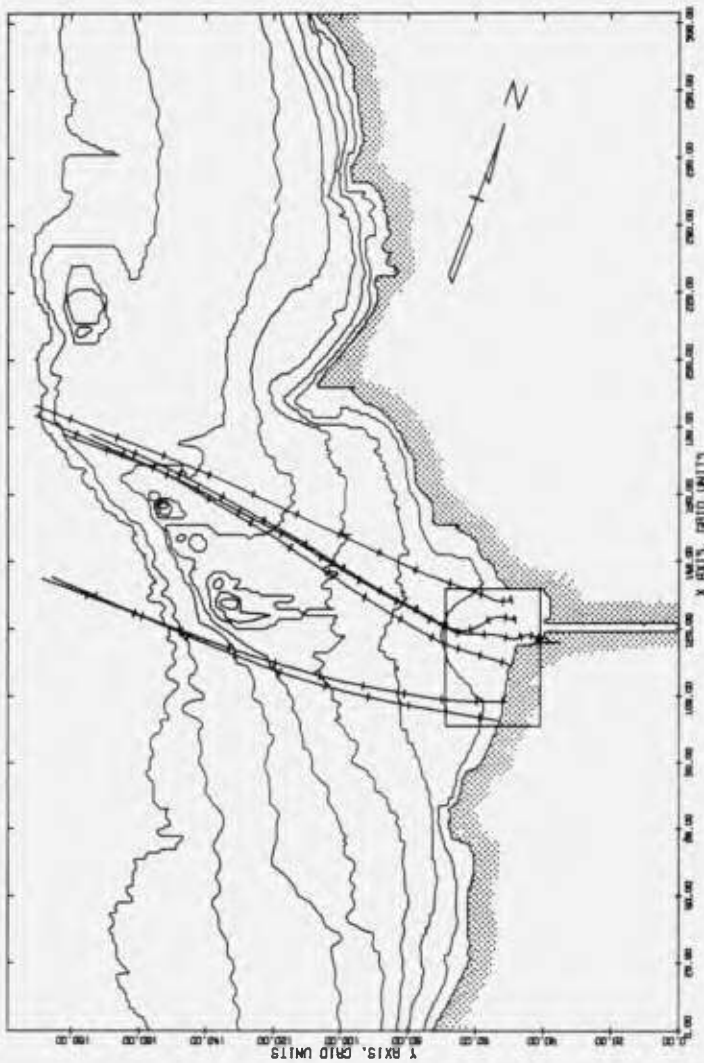


FIGURE 1A
OUTER GRID CONTOUR MAP and
13 SEC. WAVE RAYS TO STATIONS 1,2,3,4,5,7

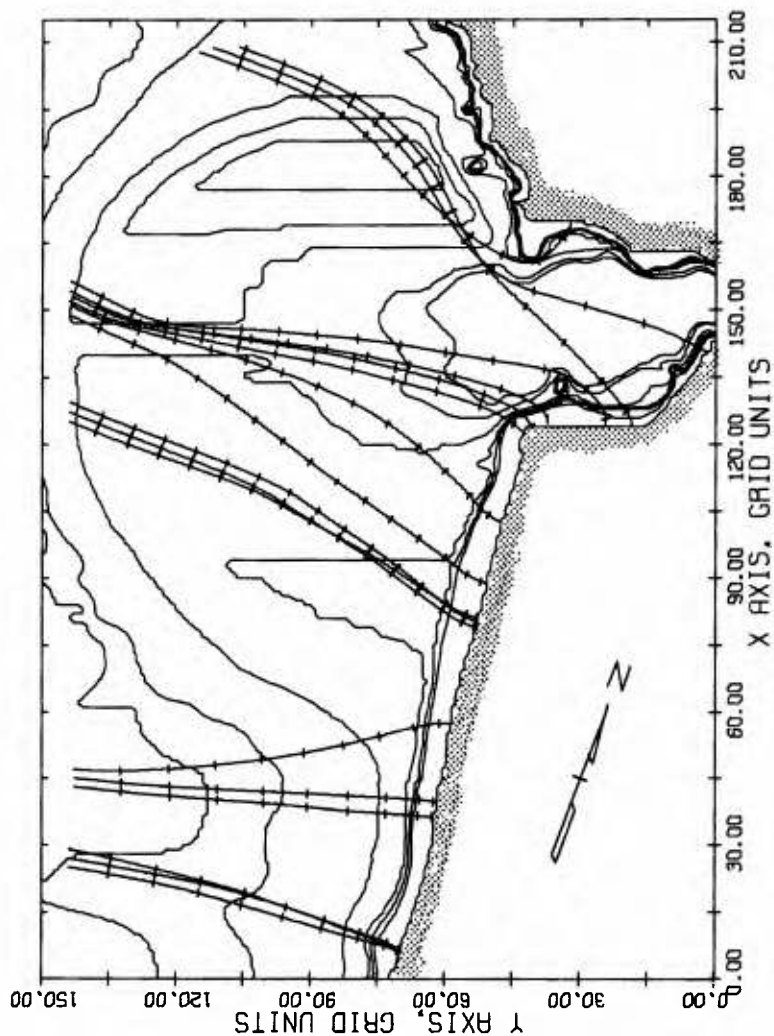


FIGURE 1B

INNER GRID CONTOUR MAP and
13 SEC. WAVE RAYS TO STATIONS 1,2,3,4,5,7

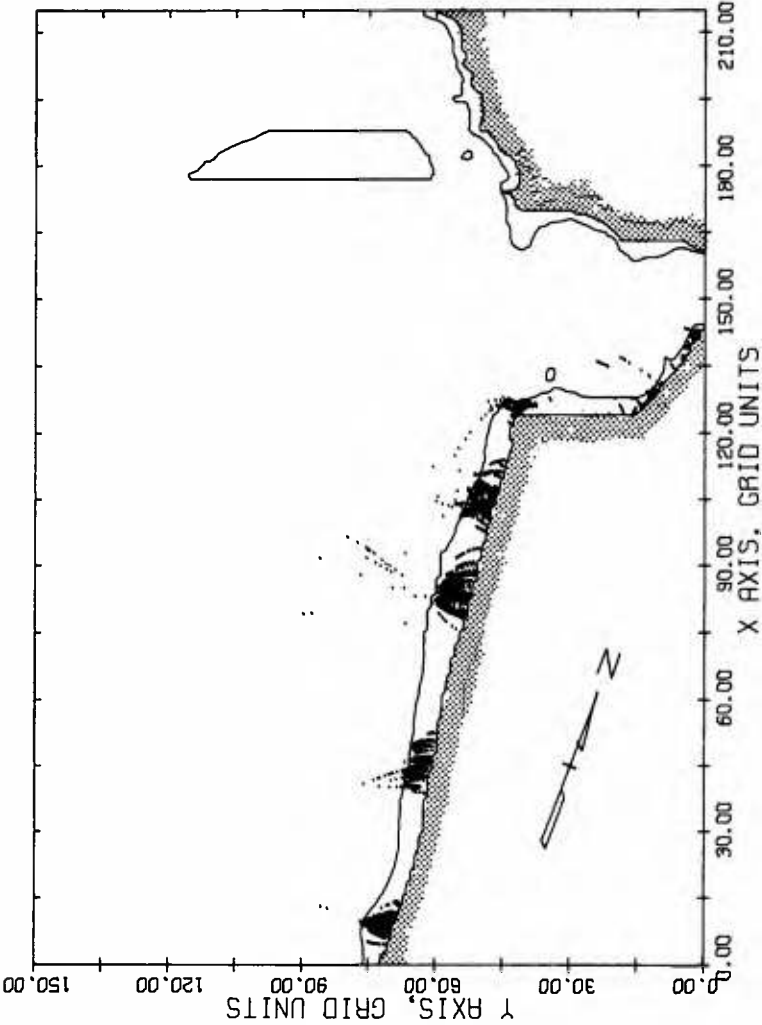


FIGURE 2

SCATTERGRAPH
Showing Breaking Locations for the Case $K_r < \infty$

